

# High density QCD at THERA

E. Gotsman<sup>a</sup>, E. Levin<sup>a</sup>, M. Lublinsky<sup>b</sup>, U. Maor<sup>a</sup>, E. Naftali<sup>a</sup> and K. Tuchin<sup>a</sup>

<sup>a</sup> *HEP Department, School of Physics and Astronomy  
Tel Aviv University, Tel Aviv 69978, Israel*

<sup>b</sup> *Department of Physics, Technion,  
Haifa, 32000, Israel*

## Abstract

These notes are a summary of our predictions for the new THERA project, related to deep inelastic scattering in the region of ultra low  $x$  ( $x \rightarrow 10^{-7}$ ). We collect here predictions that satisfy two criteria (i) they do not depend on specific features of the model that we have to use to estimate a possible effect; and (ii) they do not contradict the HERA data.

## 1 Introduction: Our hopes and main goals at THERA

### 1.1 Three domains of QCD at low $x$

Deep inelastic scattering is a unique experiment which allows us to take ‘snapshots’ of the constituents inside a hadron at different moments of time with different resolutions. These ‘snapshots’ provide the possibility of finding the degrees of freedom (DOF) that are responsible for the interaction in QCD and generalize the theoretical approach from the well defined domain of perturbative QCD to the unknown non-perturbative (confinement) region, where the appropriate theoretical methods are still to be determined. DIS allows one to see the constituents of size  $\approx 1/Q$ , where  $Q$  is the photon virtuality, at the time  $t \approx 1/mx$ , where  $x$  is the Bjorken variable related to the energy ( $W$ ) of the process ( $x = Q^2/W^2$  at low  $x$ ).

HERA data as well as theoretical studies suggest that hadrons have qualitatively diverse structure in the three different domains (see Figs. 1 and 2):

- 1. Perturbative QCD domain** where the constituents are of small size and are distributed in a hadron with rather low density (packing factor of these constituents  $\kappa$  is small ( $\kappa < 1$ , see Fig. 3));

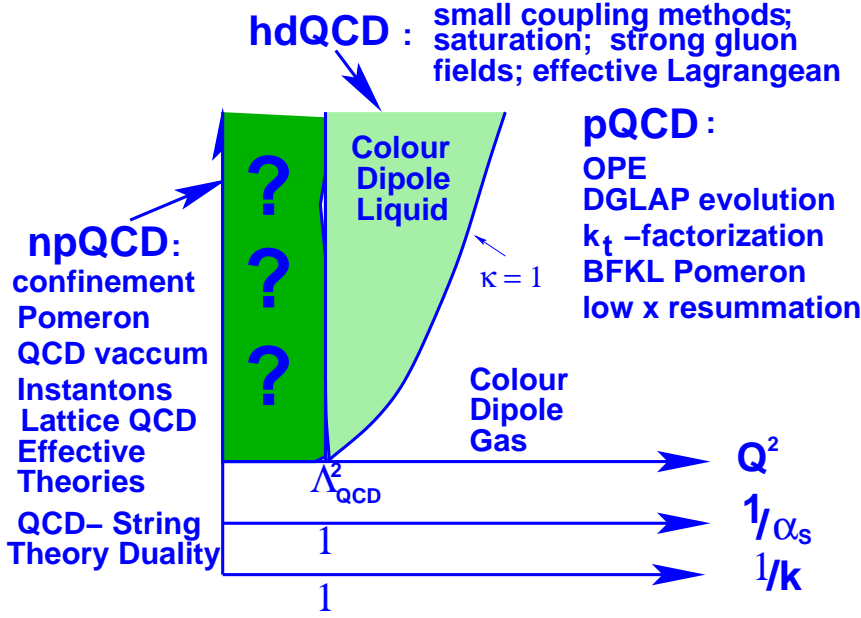


Figure 1: Phase diagram of DIS.  $\kappa$  is the packing factor which is the number of constituents multiplied by its typical area and divided by the area of a hadron.

2. **High parton density QCD domain** in which the constituents are still small and we can use weak coupling methods, but their density is so large that their packing factor  $\kappa > 1$ , and so we cannot treat this system of partons using the established pQCD methods;
3. **Non perturbative QCD domain** in which the QCD coupling is large, the confinement of quarks and gluons occurs, and new theoretical methods must be developed to explore this region.

Fig. 2 illustrates these ‘snapshots’ of the constituents at different moments of time ( different values of  $x$  ). One can see three domains with different distributions of the constituents in the transverse plane. It should be stressed that the distributions do not depend on the reference frame, unlike time which differs in different reference frames.

Each of these domains has its own theoretical problems that can be clarified by THERA experiments. The key problems are shown in Fig. 1.

## 1.2 Brief summary of HERA data

Brief resume of HERA data: these data can be described by models including parton saturation, but they can also be described without assuming saturation. However, it turns out that all predictions of asymptotic hdQCD have already been seen in HERA data. This fact is so impressive and convincing that we, personally, think that HERA has reached a new regime of high density QCD [1]. However, the situation is still non-conclusive as is illustrated by Fig. 4 which shows the value of the saturation scale in HERA and THERA kinematic region. One can see that  $Q_s(x) \leq 1 \text{ GeV}$  for HERA. This low  $Q_s(x)$  indicates that HERA data can be described by other approaches without saturation, for example, by some models that include a smooth matching between “soft” and “hard” interactions. However, at THERA  $Q_s(x)$  is larger and the hdQCD interpretation of the data will be cleaner. We illustrate this point with two figures that follow.

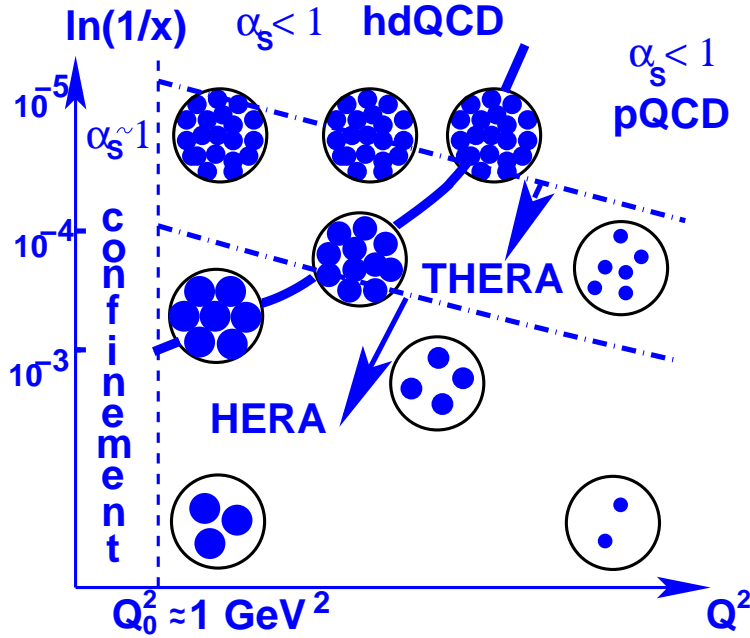


Figure 2: ‘Snapshots’ of the constituents of different size ( $r \approx 1/Q$ ) at different values of  $x$ . Large circles indicate the hadron and small ones the constituents.

### 1.3 Main idea

As we have discussed, we face two challenging problems in the region of low  $x$  and low  $Q^2$  which is now being investigated at HERA :

1. The matching of “hard” processes, which can be successfully described using perturbative QCD (pQCD), and “soft” processes, which should be described using non-perturbative QCD (npQCD);
2. Theoretical description of high density QCD (hdQCD). In this kinematic region we expect that the typical distances will be small, but the parton density will be so large that a new non perturbative approach needs to be developed for dealing with this system.

The main physical idea, on which our approach is based is [2]:

*The above two problems are correlated and the system of partons always passes through the stage of hdQCD ( at shorter distances ) before it proceeds to non-perturbative QCD and which, in practice, we describe using Reggeon phenomenology.*

### 1.4 Status of theory

Parton saturation as well as other collective phenomena typical of the high parton density system, is not an additional postulate of QCD, but follows from the QCD evolution equations in the kinematic region associated with high parton density. Therefore, it is very important to have a clear understanding what can be proven theoretically.

In DIS at low  $x$ , one can find a system of high density partons, which is a non-perturbative system due to high density of partons, although the running QCD coupling constant is still

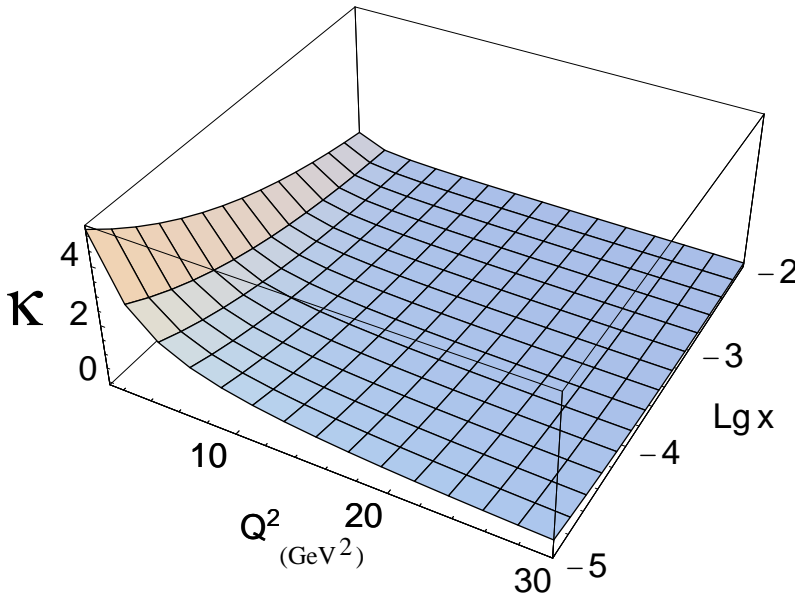


Figure 3: The parton packing factor  $\kappa$  as function of  $Q^2$  and Bjorken  $x$  in the GRV'98 parameterization of the solution to the DGLAP evolution equation. The GRV'98 parameterization describes all available data from HERA.

small ( $\alpha_S(r_\perp) \ll 1$ ). Such a unique system can be treated theoretically [2]. It should be stressed that the theory of hdQCD is now in very good shape.

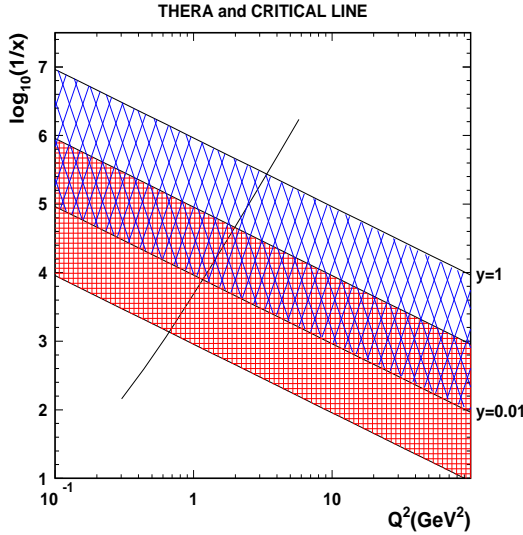


Figure 4: The estimates for the saturation scale for HERA and THERA kinematic region.

Two approaches have been developed for hdQCD. The first one [3] is based on pQCD ( see GLR and Mueller and Qiu papers in Ref. [2] ) and on dipole degrees of freedom [4]. This approach gives a natural description of the parton cascade in the kinematic region for  $\kappa \leq 1$  and up to the transition region with  $\kappa \approx 1$  ( see Fig. 2).

The second method [5] uses the effective Lagrangian suggested by McLerran and Venugopalan [2], this is a natural framework to describe data in the deep saturation region, where  $\kappa \gg 1$  (see Fig. 2). As a result of intensive work using these two approaches the non-linear evolution equation which has the following form has been derived [6]

$$\begin{aligned} \frac{da^{el}(\mathbf{x}_{01}, b_t, y)}{dy} &= -\frac{2C_F\alpha_s}{\pi} \ln\left(\frac{\mathbf{x}_{01}^2}{\rho^2}\right) a^{el}(\mathbf{x}, b_t, y) + \frac{C_F\alpha_s}{\pi} \int_{\rho} d^2\mathbf{x}_2 \frac{\mathbf{x}_{01}^2}{\mathbf{x}_{02}^2 \mathbf{x}_{12}^2} \\ &\cdot \left( 2a^{el}(\mathbf{x}_{02}, b_t, y) - a^{el}(\mathbf{x}_{02}, b_t, y) a^{el}(\mathbf{x}_{12}, b_t, y) \right), \end{aligned} \quad (1)$$

where  $a^{el}(r_{\perp}^2, b_t, x)$  is the elastic scattering amplitude for a dipole of size  $r_{\perp}$  at energy  $\propto 1/x$  and at impact parameter  $b_t$ . We assume that  $b_t \leq x_{02}$  and/or  $x_{12}$ .

The dipole cross section is equal to  $\sigma(r_{\perp}^2, x) = 2 \int d^2b_t a^{el}(r_{\perp}^2, b_t, x)$ . The pictorial form of Eq. (1) is given in Fig. 5 which shows that the physics underlying this equation has a simple meaning: the dipole of size  $x_{10}$  decays in two dipoles of sizes  $x_{12}$  and  $x_{02}$ . These two dipoles interact with the target. The non-linear term which takes into account the Glauber corrections for such an interaction, Eq. (1) is the same as the GLR -equation [2] but here it is given in the coordinate representation. The coefficient in front of the non-linear term coincides in the double log with the one calculated in Ref. [7].

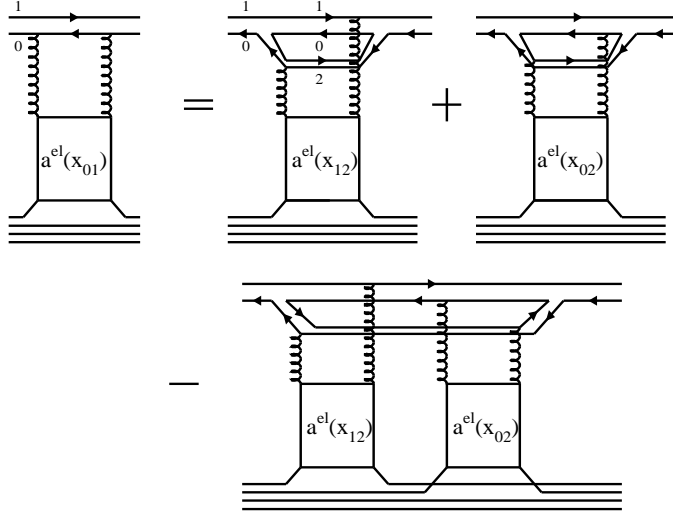


Figure 5: *The pictorial form of the non-linear evolution equation in the hdQCD kinematic region.*

We wish to stress that this equation which includes the Glauber rescatterings, has definite initial conditions and has been derived by both methods (see Refs. [6, 8]). The model, which we will describe in the next section, provides both the correct initial conditions for Eq. (1) and also serves as a good first iteration. This iteration reproduces the main features of the solution, and it is only necessary to repeat the iteration procedure two or three times to obtain a correct solution for  $x \leq 10^{-7}$ .

## 2 Our model

### 2.1 General description

As was shown in Ref. [6], the correct initial condition for Eq. (1) is actually the Glauber-Mueller formula [10, 11, 12] for the rescattering of the colour dipole, namely

$$\sigma_{dipole}(r_{\perp}, x) = 2 \int d^2b_t \text{Im} a^{el}(r_{\perp}, x; b_t), \quad (2)$$

where

$$a^{el}(r_{\perp}, x; b_t) = i \left( 1 - e^{-\frac{\Omega(r_{\perp}, x; b_t)}{2}} \right), \quad (3)$$

The opacity  $\Omega(r_{\perp}, x; b_t)$  is defined as

$$\Omega(r_{\perp}, x; b_t) = \frac{\pi^2 r_{\perp}^2}{3\pi R^2} x G^{DGLAP}(x, \frac{4}{r_{\perp}^2}; b_t), \quad (4)$$

where  $G^{DGLAP}(x, \frac{4}{r_{\perp}^2}; b_t) = G^{DGLAP}(x, \frac{4}{r_{\perp}^2}) \cdot S(b_t)$  and  $G^{DGLAP}(x, \frac{4}{r_{\perp}^2})$  is the solution of the linear DGLAP evolution equation, and  $S(b_t)$  is the profile function for the impact parameter distribution of the gluons in the target. The origin of this function is non-perturbative, and it is normalized in Eq. (4) by the condition  $S(b_t = 0) = 1$ .

For the solution of Eq. (1) one should fix the value of initial  $x = x_0$  ( $y = y_0$ ) and use  $a^{el}(r_{\perp}, x = x_0; b_t)$  as a starting iteration of Eq. (1). In our model we suggest a different approach, namely we use Eq. (2) and Eq. (3) as the first iteration of the Eq. (1) including their  $x$ -dependence. Therefore, the result of the second iteration of Eq. (1) can be written in the form:

$$a_2^{el}(r_{\perp}, y = \ln(1/x); b_t) = \frac{C_F \alpha_s}{\pi} r_{\perp}^2 \int_{r_{\perp}^2}^y dy' \int_{r_{\perp}^4} \frac{d^2 r'_{\perp}}{r'^4_{\perp}} \{ 2 a_1^{el}(r'_{\perp}, y'; b_t) - (a_1^{el}(r'_{\perp}, y'; b_t))^2 \}, \quad (5)$$

where we assumed that  $r'_{\perp} \gg r_{\perp}$ . This assumption corresponds to the Leading Log Approximation of perturbative QCD LLA, which has been used in the derivation of Eq. (2) and Eq. (3). Substituting Eq. (2) in Eq. (5) we obtain

$$a_2^{el}(r_{\perp}, y = \ln(1/x); b_t) = r_{\perp}^2 \int_{r_{\perp}^2}^y dy' \int_{r_{\perp}^4} \frac{d^2 r'_{\perp}}{r'^4_{\perp}} \left( 1 - e^{-\frac{\Omega_G(r'_{\perp}, y'; b_t)}{2}} \right), \quad (6)$$

where  $\Omega_G(r_{\perp}, y; b_t) = 2\Omega(r_{\perp}, y; b_t)$  of Eq. (4)<sup>1</sup>.

The physical meaning of Eq. (6) is transparent. The dipole of size  $r_{\perp}$  decays into two dipoles which interact with the target. Eq. (6) describes the rescatterings of these two dipoles. On the other hand, in pQCD this state is the  $q\bar{q}G$  state. Since we assume the size of  $q\bar{q}$  system to be much smaller than the size of the dipoles in the  $q\bar{q}G$  state, Eq. (6) relates to the passage of the gluon through the target. Using the relation between the gluon-target cross section<sup>2</sup> and the gluon distribution

$$\sigma^G = 2 \int d^2 b_t a_2^{el}(r_{\perp}, y = \ln(1/x); b_t) = \frac{4\pi^2}{Q^2} \alpha_s(Q^2) x G(x, Q^2)$$

one obtains the Glauber-Mueller formula for the gluon distribution [12]

$$xG^{SC}(x, Q^2) = \frac{8}{\pi^4} \int_x^1 \frac{dx'}{x'} \int_{4/Q^2} \frac{d^2 r'_{\perp}}{r'^4_{\perp}} \int d^2 b_t \left( 1 - e^{-\frac{\Omega^G}{2}} \right). \quad (7)$$

Eq. (2) and Eq. (7) are the main formulae that we use in our estimates of the collective phenomena in DIS.

<sup>1</sup>Actually,  $\Omega_G/\Omega = 2N_c^2/(N_c^2 - 1) = 9/4(N_c = 3) \rightarrow 2(N_c \gg 1)$ .

<sup>2</sup>In principle, the gluon - target cross sections can be measured using the graviton as a colourless probe.

## 2.2 Advantages and disadvantages of the model.

The main advantages of our model follow directly from the way it has been constructed. Our model reproduces the DGLAP limit for  $r_{\perp}^2 < r_{saturation}^2 \approx 1/Q_s^2$ , gives a good approximation to the solution of Eq. (1) for  $x \geq 10^{-6}$ , and it preserves the relation between elastic, quasi-elastic ( diffraction) scattering and multi particle production in DIS based on the AGK cutting rules [13] (see Ref. [1] for details).

The main problem relating to our model is the fact that the evolution equation Eq. (1) has only been proven in the leading  $\ln(1/x)$  approximation of pQCD where we consider  $\alpha_S \ln(1/x) \approx 1$  while  $\alpha_S \ll 1$ . This approximation does not insure the accuracy of calculation for present accessible energies. On the other had, our model cannot be correct at low  $x$  and it is only suitable to describe DIS for  $x \geq 10^{-6}$ , where the model gives the second iteration of Eq. (1). For smaller values of  $x$  we require higher iterations.

In Ref. [14] we have already shown that our model gives a good approximation of Eq. (1). Fig. 6 illustrates this point. Hence we can safely use our model for estimates of the collective phenomena even in THERA kinematic region.

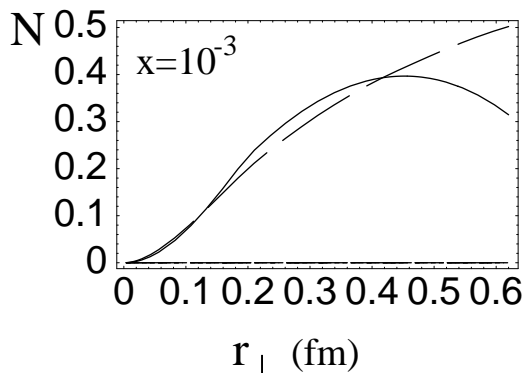


Fig.6-a

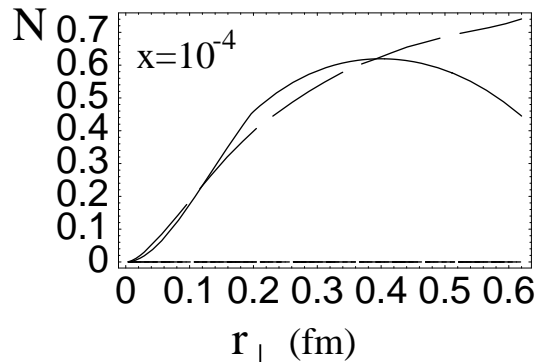


Fig. 6-b

Figure 6: *Figs.6-a - 6-b show the calculation for  $N = \text{Im } a^{el}$  at  $b_t = 0$  ( $\sigma_{dipole} = \int d^2b_t N(x, r_{\perp}; b_t)$ ) in our model ( full curve ) and the solution to nonlinear equation (see Eq. (1)).*

Table 1 provides a guide for the different processes which we described in our model for kinematical range at HERA.

## 2.3 Phenomenological parameters of the model:

Before discussing the applications at THERA we list the parameters that we use to fit the data at HERA.

<b>Table 1</b>			
Reaction	$Q^2 \text{ (GeV}^2\text{)}$	$x$	References
$\sigma_{tot}(\gamma^* p)$	$0 \div 65$	$< 0.01$	[15]
$F_2(x, Q^2)$	$1 \div 65$	$< 0.01$	[7, 17]
$xG(Q^2, x)$	$1 \div 65$	$< 0.01$	[7]
$dF_2/d\ln Q^2$	$1 \div 65$	$< 0.01$	[18, 23]
$\sigma_{tot}(\gamma \gamma^*)$	$0; 0 \div 20$	$< 0.01$	[19]
$\sigma_{tot}^{diff}$	$5 \div 65$	$< 0.01$	[20]
$\frac{\sigma_{tot}^{diff}}{\sigma_{tot}}$	$1 \div 65$	$< 0.01$	[21]
$\sigma(\gamma^* p \rightarrow J/\Psi + p)$	$0 \div 65$	$< 0.01$	[22, 23]
slope $B(\gamma^* p \rightarrow J/\Psi + p)$	$0 \div 65$	$< 0.01$	[22]
slope $B(\gamma^* p \rightarrow \rho + p)$	$5 \div 65$	$< 0.01$	[22]

### 2.3.1 $R^2$ - size of the target.

The size of the target enters the impact parameter profile of the target which we take in the Gaussian form:

$$S(b_t) = \frac{1}{\pi R^2} e^{-\frac{b_t^2}{R^2}}. \quad (8)$$

The HERA data for photo production of the  $J/\Psi$  - meson as well as CDF data on double parton cross section, leads to the value of  $R^2 = 5 \div 10 \text{ GeV}^{-2}$ .  $R^2$  is a parameter fied to describe of the experimental data. Note, that the value of  $R^2 = 8.5 \text{ GeV}^{-2}$  was taken for all reactions that we have described.

### 2.3.2 $Q_0^2 = 1/r_{sep}^2$ - separation parameter.

As we have discussed we can only rely on our model for the saturation effect ( see Eq. (2) - Eq. (3) ) at rather small distances ( $r_\perp < r_\perp^{sep}$ ) or , in other words, at large virtualities of the incoming photon  $Q^2 > Q_0^2$ . We have commented on the value of  $r_\perp^{sep}$ , but in practice we used  $Q_0^2 = 0.6 \div 1 \text{ GeV}^2$  and tried to estimate how our fit depends on the value of  $Q_0^2$ . Therefore, the result of our calculations should be read , as “*the shadowing corrections from short distances  $r_\perp < 1/Q_0^2$  gives this or that ....*”.

### 2.3.3 Solution of the DGLAP evolution equations.

We attempted to use all available parameterization of the solution of the DGLAP evolution equations[24, 25], but we prefer the GRV parameterization[26] . The reason for this is very



simple: the theoretical formulae, that are the basis of our model, were derived in double log approximation of pQCD, and the GRV parameterization is the closest one to the DLA.

### 3 Predictions for THERA

#### 3.1 The unitarity bound in THERA kinematic region

We start from the prediction which, in principle, does not depend on the exact form of the correct evolution equation and/or on the particular model, namely, from unitarity bound for  $F_2$  and  $xG(x, Q^2)$  [27]. This bound stems from a simple formula for the DIS cross section [10, 11, 12]

$$\sigma(\gamma^* p) = \int_0^1 dz \int d^2 r_\perp |\Psi(z, r_\perp; Q^2)|^2 \sigma_{dipole}(x_B, r_\perp^2), \quad (9)$$

where  $\sigma_{dipole}(x_B, r_\perp^2)$  is the total cross section of the  $q\bar{q}$ -dipole of size  $r_\perp$  with the target;  $\Psi$  is the wave function of the  $q\bar{q}$ -dipole in the virtual photon. This wave function is well known [12, 16] and for transverse polarised photon  $|\Psi_T(z, r_\perp; Q^2)|^2$  is equal

$$|\Psi_T(z, r_\perp; Q^2)|^2 = \frac{\alpha^{em} N_c}{2\pi^2} \times \sum_1^{N_f} Z_f^2 [z^2 + (1-z)^2] \tilde{Q}^2 K_1^2(\tilde{Q} r_\perp), \quad (10)$$

where  $K_1$  is the modified Bessel function,  $\tilde{Q}^2 = z(1-z)Q^2$ ,  $N_f$  is the number of massless quarks and  $Z_f$  is the fraction of the charge carried by the quark.

It was shown in Ref. [12, 27] that in the DGLAP limit the essential  $r_\perp$  in Eq. (9) are larger than  $2/Q$  ( $r_\perp > 2/Q$ ) and the integral over  $z$  can be taken, namely,

$$\int_0^1 dz |\Psi_T(z, r_\perp; Q^2)|^2 \rightarrow \frac{8}{3 Q^2 r_\perp^4}. \quad (11)$$

Finally, using the relation between the total cross section and  $F_2$  structure function

$$\sigma(\gamma^* p) = \frac{4\pi^2 \alpha^{em}}{Q^2} F_2(x_B, Q^2) \quad (12)$$

one obtains

$$F_2(x_B, Q^2) = \frac{N_c}{12\pi^3} \sum_1^{N_f} Z_f^2 \int_{\frac{1}{Q^2}}^\infty \frac{dr_\perp^2}{r_\perp^4} = \frac{N_c}{12\pi^3} \sum_1^{N_f} Z_f^2 2 \int d^2 b_t \text{Im} a_{dipole}^{el}(x_B, r_\perp; b_t) \quad (13)$$

Taking the derivative with respect to  $\ln Q^2$  and using the weak form of the unitarity constraint ( $\text{Im} a_{dipole}^{el}(x_B, r_\perp; b_t) \leq 1$ ) we obtain

$$\frac{\partial F_2(x, Q^2)}{\partial \ln Q^2} \leq \frac{Q^2 R^2}{3\pi^2}. \quad (14)$$

$R^2$  in Eq. (14) is the region of convergence for the integral over  $b_t$  in Eq. (14). In principle,  $R^2$  grows with  $x$  but model estimates [27] as well as experimental data [28] show only mild  $x$  dependence.

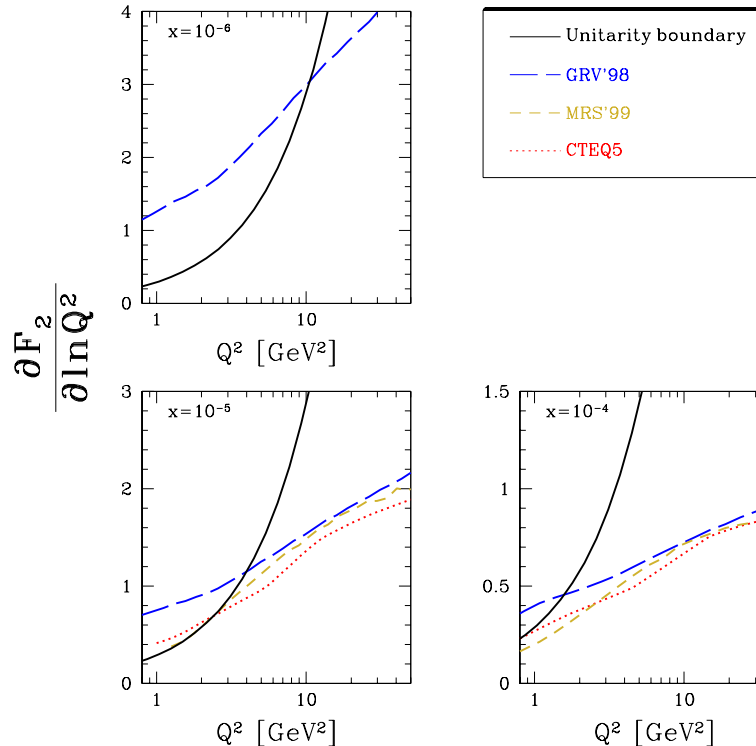


Figure 7: *The unitarity boundary and the DGLAP predictions for the  $F_2$  - slope at different values of  $x$ .*

Fig. 7 shows that the  $F_2$  slope approaches the unitarity bound at least in the GRV'98 parameterization of the solution to the DGLAP evolution equation. A violation of the unitarity bound in the DGLAP equation indicates that the shadowing corrections are unavoidable in the THERA kinematic region. The real size of these corrections is much larger than we can see from the violation of the unitarity bound, since the system starts becoming dense at densities lower than that which follows from the unitarity constraints. In other words, shadowing corrections lead to a considerable suppression in the deep inelastic structure function, at densities lower than originates from the unitarity constraints.

### 3.2 The unitarity bound for DIS with nuclei.

Eq. (14) looks better for DIS with nuclei, since the radius of the nucleus is large and a shrinkage of the diffraction peak induced by SC will be very small and we can neglect it. We plot the  $F_{2A} = AF_{2N}^{DGLAP}$  and unitarity bound in Fig. 8.

One can see that for DIS with nuclei we should see the collective phenomena at  $x \approx 10^{-4}$  and at rather large value of  $Q^2 \approx 3 \div 5 \text{ GeV}^2$ .

### 3.3 Scaling violation in the $F_2$ - slope

The careful analysis of the HERA data on the  $F_2$ - slope ( $\frac{\partial F_2(x, Q^2)}{\partial \ln Q^2}$ ), given in Ref.[18], shows that (i) our saturation model as well as other models of this type ( see [29] for example ), are able to describe all experimental data ; and (ii) such a description cannot be very conclusive since other approaches are equally successful. The saturation hypothesis leads to

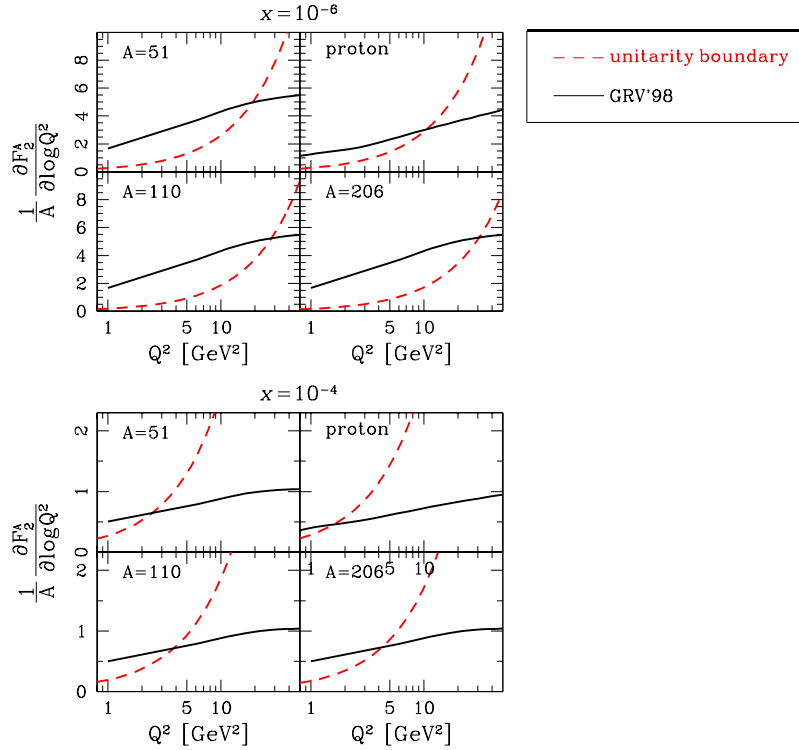


Figure 8: *The unitarity bound and the DGLAP predictions for the  $F_{2A}$  - slope at different values of  $x$  and atomic number  $A$ .*

$\frac{\partial F_2(x, Q^2)}{\partial \ln Q^2} \propto Q^2 R^2$  for  $Q^2 \leq Q_s^2(x)$ . The HERA data [30, 31] show such behaviour, but we cannot distinguish this saturation behaviour from the vanishing of  $F_2$  on the soft scale, which follows from the fact that the total photoproduction cross section is finite at  $Q^2 \rightarrow 0$ . There are two reasons for this uncertainty: (i) the soft scale is not so soft and typical transverse momentum in the soft Pomeron could be as large as  $2 \text{ GeV}$  [32]; and (ii) the saturation scale is rather small  $Q_s^2(x) = 1 \div 2 \text{ GeV}^2$  in HERA kinematic region.

One can see from Fig. 9 that THERA will allow us to distinguish between a mixture of soft and hard Pomerons (DL curve in Fig. 9) and our model for gluon saturation (GLMN curve in Fig. 9). The difference between the DGLAP approach (CTEQ5 curve in Fig. 9) and our predictions is concentrated in the region of small  $Q^2 \approx 1 \div 2 \text{ GeV}^2$ , but we recall that the corrections to the CTEQ5 parametrization due to high parton density effects reaches the value of about 30-40% at THERA energies. These estimates are an alternative way of saying, that at THERA energies we expect large SC theoretically, and a DGLAP approach can absorb these corrections in the initial nonperturbative gluon distributions at HERA energies, but it would be a more difficult task in THERA kinematic region.

### 3.4 Energy dependence of $J/\Psi$ production.

It was shown in [33, 23, 34] that the energy behaviour of the  $J/\Psi$  production is very sensitive to the value of the shadowing corrections. It turns out that the large uncertainties due to our poor knowledge of the wave function of vector mesons contribute mostly in the normalization of the cross section, while the energy slope is still a source of the information on SC. In Refs. [23, 34] we showed that the shadowing corrections provide a natural explanation of the

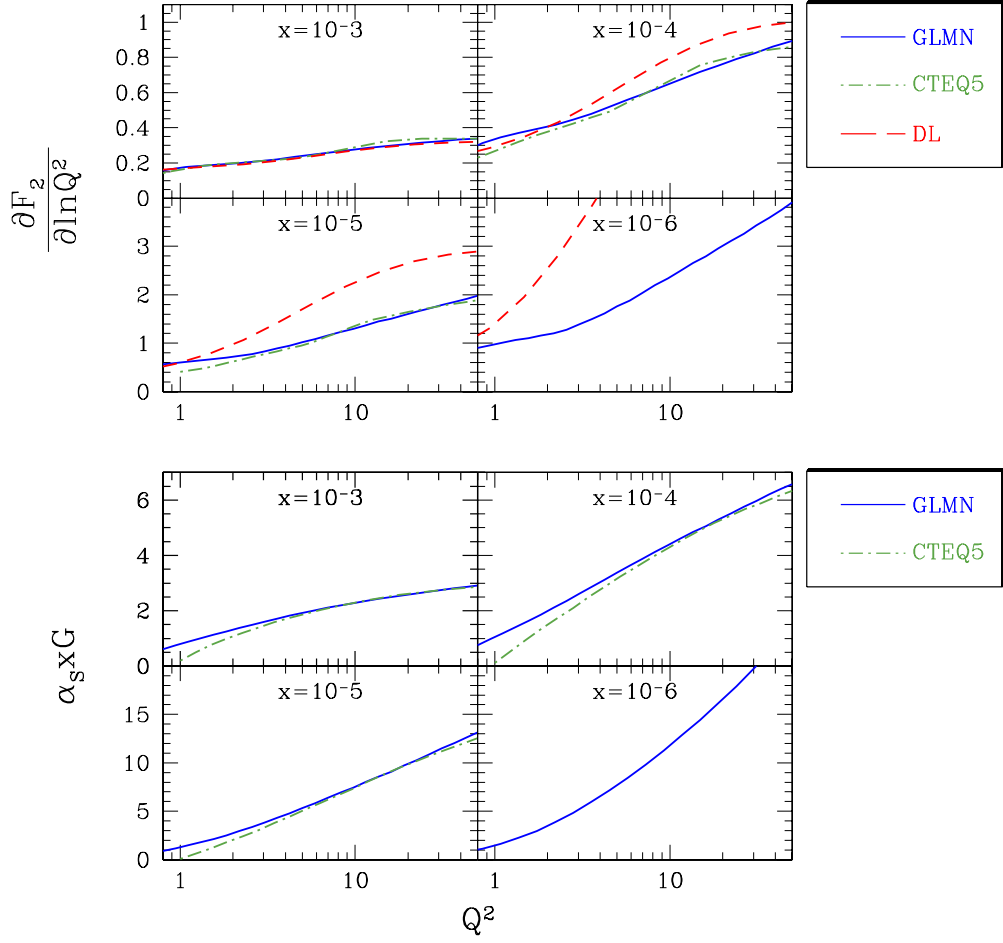


Figure 9: *Predictions for the different parameterizations at fixed low values of  $x$ .*

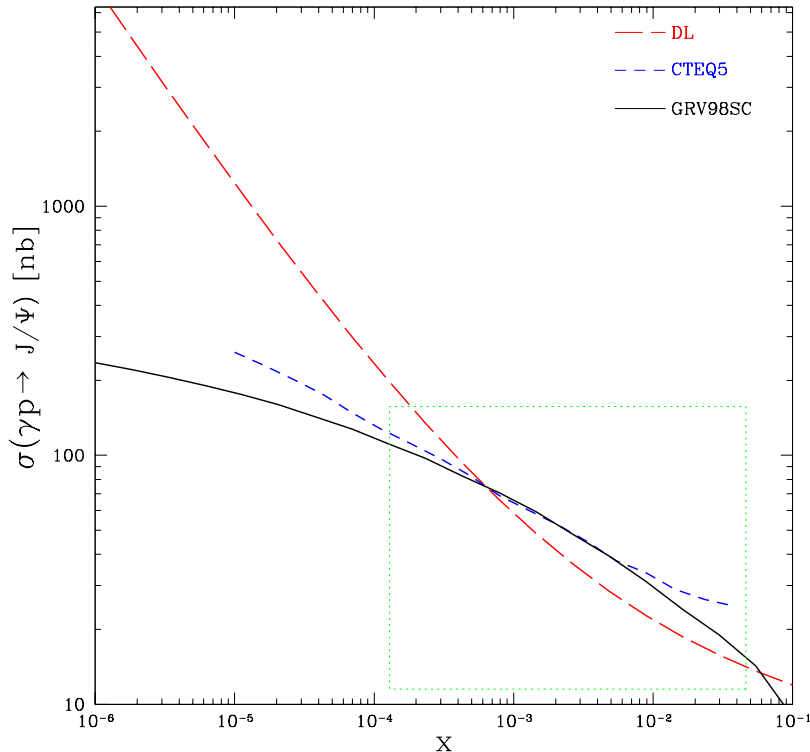


Figure 10: A comparison between the energy dependence of different models (see text) for the integrated cross section of  $J/\Psi$  photoproduction. The available experimental data points are confined within the inner window.

experimental energy behaviour for  $J/\Psi$  photo and deep inelastic production. However, the available data do not enable us to exclude explanations based on the mixture of soft and hard Pomerons, and the idea that this process is hard. Fig. 10 gives our prediction for THERA kinematic region for three approaches: the SC calculations in our model (GRV98SC), the soft + hard Pomeron model (DL2P)[35] and the DGLAP approach based on the CTEQ parametrization (CTEQ5NSC).

### 3.5 Shrinkage of diffraction peak for production of vector mesons.

The experimentally observed shrinkage of the diffraction peak in photoproduction of  $J/\Psi$ [37] is a direct indication that this process is not a simple hard process that can be described in the DGLAP approach. Indeed, one of the most well established properties of the hard processes is the fact that the  $t$ -dependence is independent of energy ( $x$ ) (see for example Ref. [22]. There are two possible explanations: (i) the first one is the SC which lead to  $x$ -dependence of the  $t$ -slope[22] and (ii) the second is based on the contamination of the  $J/\Psi$  production by the soft processes for which the shrinkage of the diffraction peak is a phenomenon that is well established both theoretically and experimentally.

It should be stressed that the above two approaches have different predictions for the  $x$ -dependence: SC lead to the  $t$ -slope which increases at higher energies (lower  $x$ ), since the contribution of SC grows with energy. For the mixture of soft and hard processes, the role of soft ones diminishes at higher energies, and as a result the value of effective  $\alpha'_{eff}$  decreases [36].

In Fig. 11 one can see this effect for our model. This figure also shows that we cannot

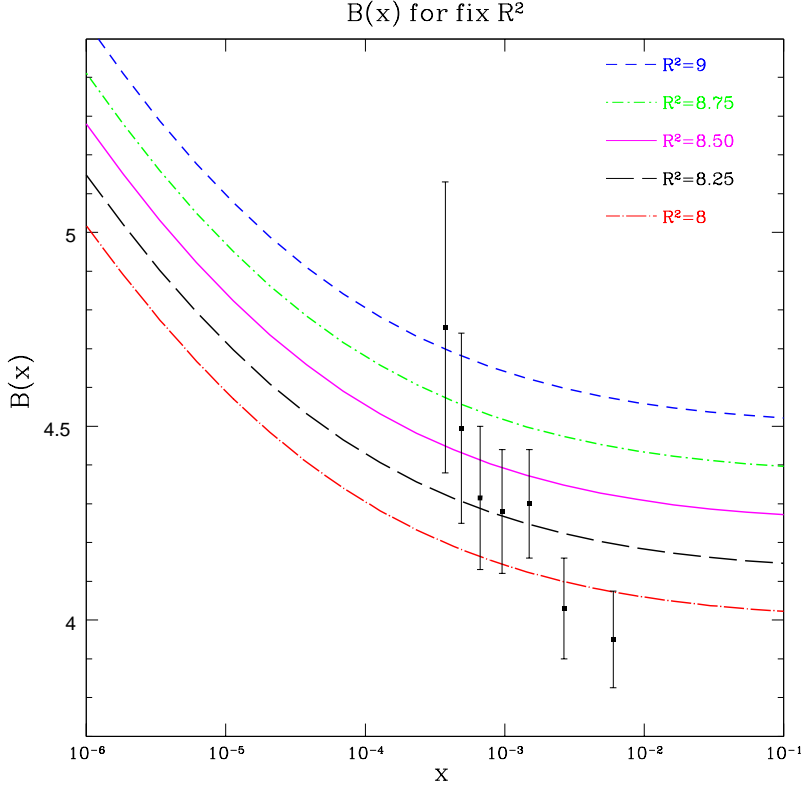


Figure 11: *The energy ( $x$ ) dependence of the forward differential slope of  $J/\Psi$  photoproduction. ZEUS data [37] and our model calculation with several values of  $R^2$ . From this picture we chose the value of  $R^2 = 8.5 \text{ GeV}^{-2}$  for the typical proton size in our model.*

describe the ZEUS data regarding the value of the  $t$ -slope. The reason for this may be due to our under estimating the value of SC in our model. However, one lesson we can learn from Fig. 11: THERA will clarify the question which mechanism works. The important thing to emphasize once more is that the measurement of the shrinkage of the  $t$ -slope will provide reliable information on the deviation from the simple DGLAP approach. It is especially important to observe such shrinkage in the DIS diffraction production of  $J/\Psi$  and other vector mesons.

### 3.6 Maxima in ratios

Preparing this paper we tried to find improved observables which will be sensitive to the saturation scale. We study the  $Q^2$  behaviour of the ratios:  $F_L/F_T$  and  $F_L^D/F_T^D$  for longitudinal and transverse structure function for inclusive DIS and for diffraction in DIS [38]. In Fig. 12 some examples of these ratios are plotted. We found that these ratios have maxima at  $Q^2 = Q_{max}^2(x)$  which increases with  $x$  as  $x \rightarrow 0$ . It appears that  $Q_{max}(x)$  is a simple function of the saturation scale  $Q_s(x)$ . In the THERA kinematic region  $Q_{max}^2(x)$  is large  $Q_{max}^2(x) \approx 6 \div 7 \text{ GeV}^2$ . Such a large value of  $Q_{max}^2(x)$  makes our calculation more reliable, and we expect that the measurement of this maxima in the THERA kinematic region will enable us to extract the value of the saturation scale from the experimental data.

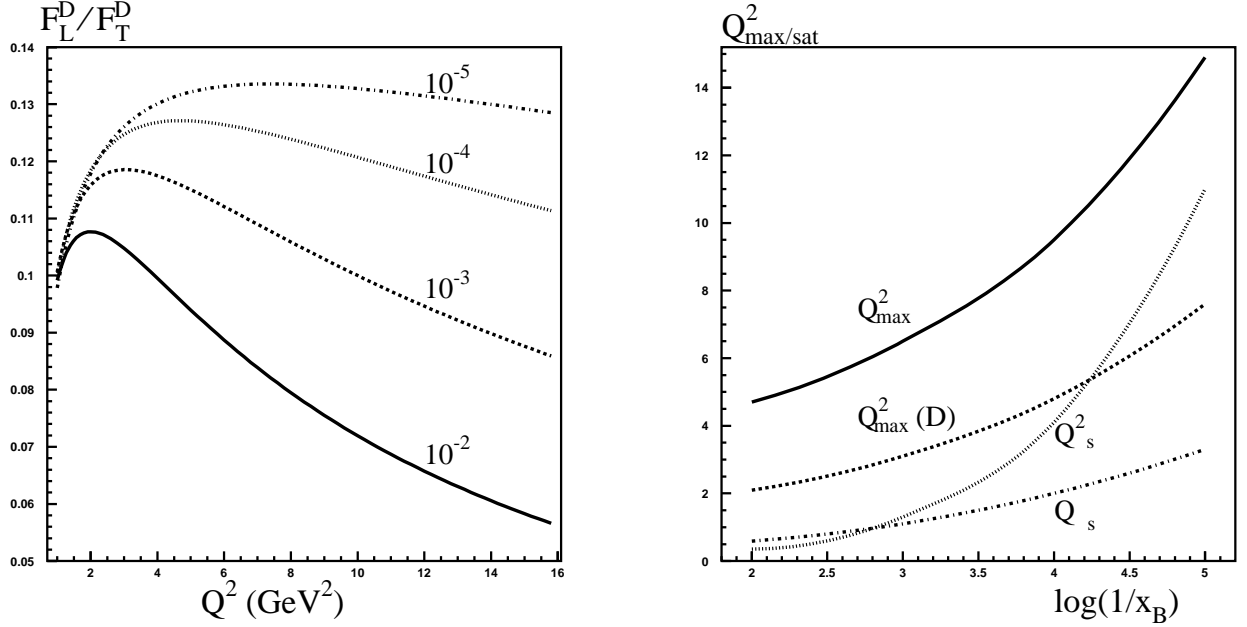


Figure 12: The ratio of  $F_L^D/F_T^D$  as function of  $Q^2$  at different values of  $x$  and the behavior of  $Q_{\max}^2(x)$  as function of  $x$ .

### 3.7 Higher twist contribution.

One of the most challenging problem of QCD is to understand the higher twist contributions. The present approach to DIS is based on two main ideas: (i) the DGLAP evolution equation for leading twist contributions and (ii) the firm belief that higher twist contributions are small in the whole kinematic region, when we start QCD evolution from the large value of  $Q^2 = Q_0^2 \approx 1 - 4 \text{ GeV}^2$ . In recent years it has been proven that there is no ground for such an assumption. It was found [39] that the anomalous dimension for the higher twists is much larger than for the leading one in the region of low  $x$ . It turns out that if we write the deep inelastic structure function in the form

$$F_2(x, Q^2) = F_2^{LT}(x, Q^2) + \frac{M^2}{Q^2} F_2^{HT}(x, Q^2)$$

$F_2^{HT}(x, Q^2) \propto F_2^{LT}(x, Q^2) \times xG(x, Q^2)$  at  $x \rightarrow 0$ . Therefore, the experimental observation of the higher twist contribution, is one of the most challenging and important problems in DIS, as well as in QCD at large. The attractive feature of our model is the fact that it leads to higher twist contributions in accord with known theoretical information. Our calculations confirm the result of Ref. [40] that there is almost a full cancellation of the higher twist contributions in  $F_2$  in spite of the fact that they give substantial contributions separately to  $F_L$  and  $F_T$  as well as to  $F^D$ . In the THERA kinematic region ( at  $x \approx 10^{-5}$ ) we expect the higher twist contributions to be of the same order as the leading twist at sufficiently high value of  $Q^2$  (see Fig. 13) This high value of  $Q^2$  insures us that our calculations are reliable. Therefore, we believe that THERA has a good chance to measure higher twist terms and a new era of DIS will open, that will include a systematic study of higher twist contributions.

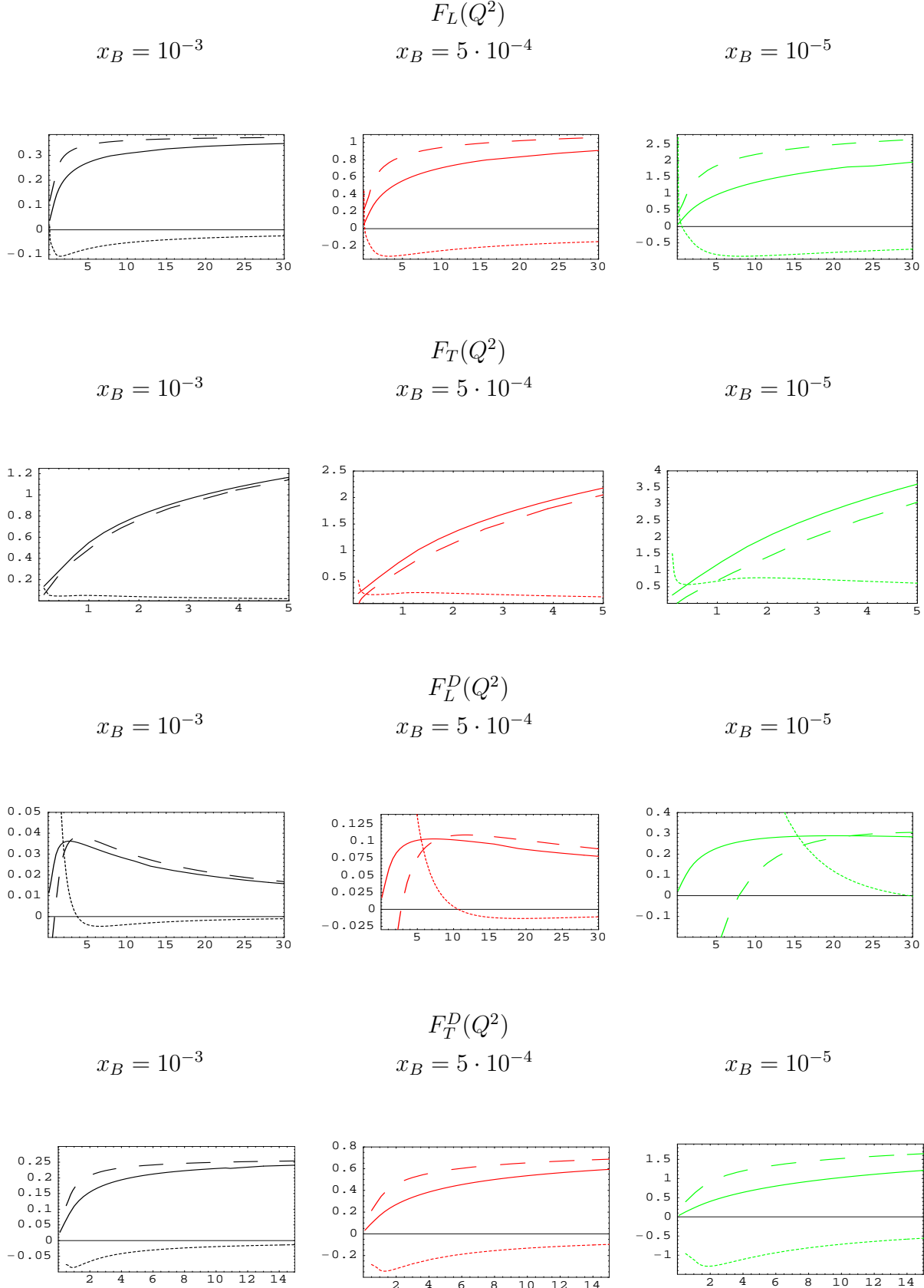


Figure 13: *Different twist contributions to the various structure functions for DIS on the proton: leading twist (at high  $Q^2$ ) – dashed line, next-to-leading – dotted one, exact structure function – solid curve.*



## 4 Resume

We presented here our estimates for the possible manifestation of saturation in the THERA kinematic region. We believe that HERA has reached a new QCD regime: the high parton density QCD domain [1], where incorporating new collective phenomena is essential for understanding its physics. We argue here that data from THERA will be able to show that we have reached this new regime, and will allow a systematic study of the QCD parton system with large parton density.

We hope that our estimates will help to plan the experimental strategy for the THERA project.

## Acknowledgements

The authors are very much indebted to our coauthors and friends with whom we discussed our approach on a everyday basis Ian Balitsky, Jochen Bartels , Krystoff Golec Biernat, Larry McLerran, Dima Kharzeev, Yuri Kovchegov and Al Mueller for their help and fruitful discussions on the subject. E.G. , E. L. U.M. and K.T. thank BNL Nuclear Theory Group and DESY Theory group for their hospitality and creative atmosphere during several stages of this work.

This research was supported in part by the BSF grant # 9800276, by the GIF grant # I-620-22.14/1999 and by Israeli Science Foundation, founded by the Israeli Academy of Science and Humanities.

## References

- [1] E.Gotsman et al., “*Has HERA reached a new QCD regime?*”, DESY 00-19,TAUP-2649-200, hep-ph/001019.
- [2] L.V. Gribov, E.M. Levin and M.G. Ryskin, *Phys. Rep* **100** (1983) 1;  
A.H. Mueller and J. Qiu, *Nucl. Phys.* **B268** (1986) 427;  
L. McLerran and R. Venugopalan, *Phys. Rev.* **D49** (1994) 2233,3352, **50** (1994) 2225, **53** (1996) 458, **59** (1999) 094002.
- [3] E. Levin and M.G. Ryskin, *Phys. Rep.* **189** (19267) 1990;  
J.C.Collins and J. Kwiecinski, *Nucl. Phys.* **B335** (1990) 89;  
J. Bartels, J. Blumlein and G. Shuler, *Z. Phys.* **C50** (1991) 91;  
E. Laenen and E. Levin, *Ann. Rev. Nucl. Part. Sci.* **44** (1994) 199 and references therein;  
A.L. Ayala, M.B. Gay Ducati and E.M. Levin, *Nucl. Phys.* **B493** (1997) 305, **B510** (1990) 355;  
Ia. Balitsky, *Nucl.Phys.* **B463** (1996) 99;  
Yu. Kovchegov, *Phys. Rev.* **D54** (191996) 5463, **D55**(1997) 5445, **D60**(2000) 034008, **D61** (2000)074018;  
A.H. Mueller, *Nucl. Phys.* **B572**(2000)227, **B558** (1999) 285;  
Yu. V. Kovchegov, A.H. Mueller, *Nucl. Phys.* **B529** (1998) 451;  
E. Levin and K. Tuchin, *Nucl. Phys.* **B573**(2000) 833.

- [4] A.H. Mueller, *Nucl. Phys.* **B415** (1994) 373.
- [5] J. Jalilian-Marian, A. Kovner, L. McLerran and H. Weigert, *Phys. Rev.* **DD55** (1997) 5414;  
 J. Jalil H. Weigert, NORDITA-2000-34-HE, hep-ph/0004044. J. JuliLian-Marian, A. Kovner and H. Weigert, *Phys. Rev.* **D59** (1999) 014015;  
 J. Jalilian-Marian, A. Kovner and H. Weigert, *Phys. Rev.* **D59** (1999) 014015;  
 J. Jalilian-Marian, A. Kovner, A. Leonidov and H. Weigert, *Phys. Rev.* **D59** (1999) 014014,034007, Erratum-ibid. *Phys. Rev.* **D59** (1999) 099903;  
 A. Kovner, J.Guilherme Milhano and H. Weigert, OUTP-00-10P,NORDITA-2000-14-HE, hep-ph/0004014;  
 H. Weigert, NORDITA-2000-34-HE, hep-ph/0004044.
- [6] Ia. Balitsky, *Nucl.Phys.* **B463** (1996) 99; Yu. Kovchegov, *Phys. Rev.* **D60** (191000) 034008.
- [7] A.L. Ayala, M.B. Gay Ducati and E.M. Levin, *Nucl. Phys.* **B493** (1997) 305, **B510** (1998) 355.
- [8] E. Iancu, A. Leonidov and L. McLerran, “Nonlinear Gluon Evolution in the Color Glass Condensate: I”, Saclay - T00/166, BNL-NT-00/24, hep-ph/0011241.
- [9] Yu. V. Kovchegov, *Phys. Rev.* **D61** (2000) 074018;  
 E. Levin and K. Tuchin, *Nucl.Phys.* **B573** (2000) 833;  
 M. Braun, *Eur.Phys.J.* **C16** (2000) 337.
- [10] A. Zamolodchikov, B. Kopeliovich and L. Lapidus, *JETP Lett.* **33** (1981) 595;
- [11] E.M. Levin and M.G. Ryskin, *Sov. J. Nucl. Phys.* **45** (1987) 150.
- [12] A. H. Mueller, *Nucl. Phys.* **B335** (1990) 115.
- [13] V.A. Abramovsky, V.N. Gribov and O.V. Kancheli, *Sov. J. Nucl. Phys.* **18** (1974) 308.
- [14] M. Lublinsky, E. Gotsman, E. Levin and U. Maor, “Nonlinear Evolution and Deep Inelastic Structure Functions at LHC Energies”, in preparation.
- [15] E. Gotsman, E. Levin, U. Maor and E. Naftali, *Eur.Phys.J.* **C10** (1999) 689;  
 E. Gotsman, E. Levin and U. Maor, *Eur.Phys.J.* **C5** (1998) 303.
- [16] N.N. Nikolaev and B.G. Zakharov, *Z. Phys.* **C49** (1991) 607;  
 E.M. Levin, A.D. Martin, M.G. Ryskin and T. Teubner, *Z. Phys.* **C74** (1997) 671.
- [17] E. Gotsman, E. Levin and U. Maor, *Phys.Lett.* **B379** (1990) 186.
- [18] E. Gotsman, E. Levin, U. Maor and E. Naftali, *Nucl.Phys.* **B539** (1999) 535;  
 E. Gotsman, E. Levin and U. Maor, *Phys.Lett.* **B425** (1998) 369;  
 E. Gotsman, E. Ferreira, U.Maor and E. Naftali, “Scaling violations in the  $Q^2$  logarithmic derivative of  $F_2$ ”, TAUP 2653-2000,hep-ph/0011257.
- [19] E. Gotsman, E. Levin, U. Maor and E. Naftali, *Eur.Phys.J.* **C14** (2000) 511.

- [20] E. Gotsman, E. Levin and U. Maor, *Nucl.Phys.* **B493** (1997) 354.
- [21] E. Gotsman, E. Levin, M. Lublinsky, U. Maor and K. Tuchin, “*Energy dependence of  $\frac{\sigma^{DD}}{\sigma_{tot}}$  in DIS and shadowing corrections*”, TAUP-2639-2000, Jul 2000, hep-ph/0007261.
- [22] E. Gotsman, E. Levin and U. Maor, *Phys.Lett.* **B403** (1997) 120; *Nucl.Phys.* **B464** (1996) 251;  
E. Gotsman, E. Ferreira, U.Maor and E. Naftali, “*Screening corrections in photo and DIS production of  $J/\Psi$* ”, TAUP 2650-2000, hep-ph/0101142.
- [23] E. Gotsman, E. Ferreira, E. Levin, U. Maor and E. Naftali, “*Screening corrections in DIS at low  $Q^2$  and  $x$* ”, Talk given at 30th International Conference on High-Energy Physics (ICHEP 2000), Osaka, Japan, 27 Jul - 2 Aug 2000, hep-ph/0007274.
- [24] H. L. Lai et al., *Eur. Phys. J.* **C12** (2000) 37;
- [25] A. D. Martin, R. G. Roberts, W. J. Stirling and R. S. Thorne, *Eur. Phys. J.* **C4** (1998) 463.
- [26] M. Gluck, E. Reya and A. Vogt, *Eur. Phys. J.* **C5** (1998) 461.
- [27] A.L. Ayala Filho, M.B. Gay Ducati and E.M. Levin, *Phys.Lett.* **B388** (1996) 188.
- [28] H1 collaboration: S. Aid et al., *Nucl. Phys.* **B470** (1996) 3; C, Adolf et al., *Nucl. Phys.* **B497** (1997) 3;  
ZEUS collaboration: M. Derrick et al., *Z. Phys.* **C72** (1996) 399; J. Breitweg et al., *Phys. Lett.* **B407** (1997) 432; DESY-00-071, hep-ex/0005018;  
A. M. Cooper-Sarkar, R. C. E. Devenish and A. De Roeck, *Int. J. Mod. Phys.* **A13** (1998) 33;  
H. Abramowicz and A. Caldwell, *Rev. Mod. Phys.* **71** (1999) 1275.
- [29] K. Golec-Biernat and M. Wusthoff, *Phys. Rev.* **D59** (1999) 014017; **D60** (1999) 114023;  
K.Golec-Biernat, Talk at 8th International Workshop on Deep Inelastic Scattering and QCD (DIS 2000), Liverpool, England, 25-30 Apr 2000, hep-ph/0006080.
- [30] M. Klein (H1 collaboration), “*Structure Functions in Deep Inelastic Lepton-Nucleon Scattering*” Talk at Lepton-Photon Symposium, Stanford, August 1999, hep-ex/0001059.
- [31] B. Foster (ZEUS Collaboration), Invited talk, Royal Society Meeting, London, May 2000;  
ZEUS collaboration: J. Breitweg et al., *Phys. Lett.* **B487** (2000) 53.
- [32] D. Kharzeev and E. Levin, *Nucl.Phys.* **B578** (2000) 351;  
Yu. Kovchegov, D. Kharzeev and E. Levin, “*QCD instantons and the soft Pomeron*”, BNL-NT-00-18, TAUP-2637-2000, Jul 2000, hep-ph/0007182 ;  
B.Z. Kopeliovich, I.K. Potashnikova, B. Povh and E. Predazzi, *Phys.Rev.Lett.* **85** (2000) 507.
- [33] M.G. Ryskin, R.G. Roberts, A.D. Martin and E.M. Levin, *Z. Phys.* **C76** (1997) 71.

- [34] A.C. Caldwell and M.S. Soares, “ *Vector Meson Production in the Golec-Biernat Wusthoff Model*”, [hep-ph/0101085](#).
- [35] A. Donnachie and P.V. Landshoff: *Phys. Lett.* **B437** (1998) 408; *Phys. Lett.* **B470** (1999) 243.
- [36] M. McDermott, L. Frankfurt, V. Guzey and M. Strikman, “*Unitarity and the QCD-improved dipole picture*”, [hep-ph/9912547](#)
- [37] ZEUS collaboration: J. Breitweg et al., *Eur. Phys. J.* **C14** (2000) 213.  
H1 Collaboration: C. Adloff et al., *Phys. Lett.* **B483** (2000) 36.
- [38] E. Gotsman, E. Levin, L. McLerran and K. Tuchin, “*Higher twists and maxima for DIS on proton in high density QCD*”, TAUP-2644-2000, BNL-NT-00-20, Aug 2000, [hep-ph/0008280](#).
- [39] J. Bartels, *Phys. Lett.* **B298** (1993) 204, *Z. Phys.* **C60** (1993) 471;  
E.M. Levin, M.G. Ryskin and A.G. Shuvaev, *Nucl. Phys.* **B387** (1992) 589.
- [40] B. Badelek and J. Kwiecinski, *Phys. Lett.* **B418** (1998) 229 and references therein;  
J. Bartels, K. Golec-Biernat and K. Peters, “*An estimate of higher twist at small  $x_B$  and low  $Q^2$  based upon a saturation model*”, DESY-00-038, Mar 2000, [hep-ph/0003042](#).